Developing a Finite Element Head Model for Impact Simulation in Abaqus

P.G. Young[1], S.M. Qidwai[2], A. Bagchi[2], N. Kota[2], C. Pearce[3], R.T. Cotton[1]

[1]Simpleware Ltd.
[2] US Naval Research Laboratory
[3]Atkins Ltd.

Abstract: *A computational model of the human head has been developed by Simpleware and the U.S. Naval Research Laboratory (NRL) to simulate head impact. The head model was generated using high-resolution scan data, segmentation and image-based meshing techniques, and has been used in Abaqus for a range of simulations. The NRL/Simpleware head model addresses several key limitations of existing techniques for head impact modelling, most notably mesh adaptability for different applications. This paper will focus on the development of the modeling techniques used to create the NRL/Simpleware head model, and its use in Abaqus/Explicit to demonstrate accuracy and feasibility against a widely used experimental benchmark in impact loading and through investigation of potential brain injury under blast overpressure loading.*

Keywords: *Abaqus, Abaqus/Explicit, Biofidelic, Blast Impact, Blunt Impact, Brain Injury, CAD, FEA, Finite Element Method, Head Impact, Head Model Mesh Generation, Image Segmentation, Simpleware, Military. MRI Scan, Traumatic Brain Injury, US Naval Research Laboratory, and Visualization.*

1. Introduction

Accurate finite element (FE) head models generated from scan data can be used to simulate a range of head and brain injuries in Abaqus software. Traumatic Brain Injury (TBI) from head impact is a serious issue across areas such as sports, the military and general accident treatment. For example, amongst surviving casualties of the Iraq and Afghanistan wars, between 14% and 20% suffer from TBI's that result in long-term neurological and motor disorders (US Department of Veterans Affairs). While significant experimental research has been carried out into the mechanisms that cause TBI from impact or blast, these tend to be costly or limited by the availability of cadavers, suitable animal samples and other in vivo cases.

Numerical modelling using the FE method and 3D image data (MRI, CT, micro-CT…) is growing in popularity as a solution for researching TBI. However, to date methods for generating realistic human head models have included some limitations that reduce model flexibility and the speed by which they can be produced. This paper outlines a new method and applications for a computational head and neck model that promises new breakthroughs in numerical TBI-related research using solvers such as Abaqus.

2. Benefits of an Image-Based FE Method for Head Modelling

Advances in computational power and imaging techniques have contributed towards the growing effectiveness of image-based FE simulation. In terms of head modelling, FE simulation allows complex trauma mechanisms from impacts and blasts to be researched from scanned images, and offers potential for running repeatable simulations that can go hand-in-hand with other experimental tests. The major challenge of FE-based head modelling, however, involves accurately reproducing the geometry of an original scan.

Past approaches to building a computational head model typically involved manual generation of structures using Computer-aided design (CAD) tools, followed by meshing and export to a FE solver. However, CAD methods create problems in terms of reconstructing the complex anatomy of the head and internal structures, which can require a large amount of manual fixing. In this scenario, CAD-based head models are prone to error, particularly when it comes to the ability and experience of the user building the model. In addition, models built using CAD techniques often become computationally intractable as new levels of geometric fidelity are targeted.

By comparison, image-based modelling techniques that work with image data provide a faster and often more robust route to simulation. Image-based meshing techniques that work with volume scan data, such as computed tomography (CT) or magnetic resonance imaging (MRI), can generate FE meshes using full and semi-automated techniques. The particular methods outlined in this paper reduce user input to a minimum and produces meshes that are accurate, robust and include multiple complex geometries and parameters for simulation.

This approach builds upon and improves previous efforts to generate FE meshes from image data that, while successful in creating models, have experienced challenges in adapting models to new applications. For example, work has been carried out into generating a model from 14 cross-sectional MRI image slices. Image processing tools highlighted the skull, with outlines read by a C++ code and converted into CAD coordinate and spline data (Mehta et al, 1997). The resulting model provided a good approximation of the complex anatomy of the skull. Subsequent research has focused on taking advantage of developments in imaging and computational power to generate high-quality head models.

Examples include the Simulated Injury Monitor (SIMon) FE model, which was developed by the US National Highway Traffic Safety Administration. CT data representing the average adult male was used to build the mesh, with the head model having since been validated against different types of experimental data. The drawback of this model is that it was designed for a specific set of inputs, namely crash impact (Takhounts et al, 2008). Other head models include those created from T1-weighted MRI data), with diffusion tensor imaging used to inform an anisotropic material model including neural tissue (Kraft et al, 2012). A number of other models have been generated using image-based and CAD techniques, with examples including work carried out at the University of Illinois (Chen and Ostoja-Starzewski, 2010).

While these examples demonstrate advances in generating models from image data, they share the problem of being ‘fixed’ meshes that cannot be easily adapted to new applications. Users wanting to refine meshes or add in new structures such as helmets or soft and hard tissue have to carry out work directly on meshes. As well as creating a high risk of error, the resulting models are typically unsuitable for adaptation to a specific application or as tools for different validation inputs.

The NRL-Simpleware head model described in this paper solves these problems by using novel image-based meshing techniques to create a far more flexible head model than previous efforts; meshes can be generated to suit both specific problems, and can be adapted to changes in computational resources. Rather than working with pre-defined meshes, this approach generates FE meshes from pre-segmented image data. As a result, the NRL-Simpleware head model represents a cutting-edge solution for rapidly and accurately generating meshes that can be tailored to particular simulation tasks in Abaqus and other solvers. The rest of this paper outlines the development of the techniques used to produce the pre-segmented data and the creation of a particular NRL-Simpleware model for use in blast loading and blunt impact simulations in Abaqus/Explicit.

3. NRL-Simpleware Head Model Development

Step 1: Data Acquisition: Image data for the head model was obtained from a whole head in vivo MRI scan of a 25-year old male volunteer at the Exeter MR Centre, UK. The T1-weighted scan resulted in coronal plane image slices with a resolution of 1.03516 mm x 1.03516 mm, with a slice-to-slice separation of 1.04001 mm. The volunteer was 1.8 m tall and 81 kg, putting him close to the American 50th percentile male.

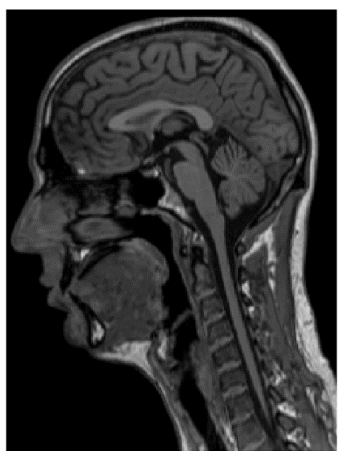

Figure 1. MRI image data used to develop the NRL-Simpleware model.

Step 2: Image segmentation: The segmentation process involved importing the DICOM (Digital

Imaging and Communications in Medicine) image series from the MRI scanner into image processing software ScanIP (Simpleware Ltd., Exeter, UK). Segmentation then entailed identifying and labelling regions of interest (ROI's) within the greyscale data, including brain, skull and muscles, as masks used for reconstructing surfaces and generating volume meshes. A range of image processing techniques were used within ScanIP to build the masks, including image threshold and flood-fill algorithms to obtain initial geometries for major structures of the head. Manual segmentation was also used to disconnect neighbouring regions with similar greyscale values.

Segmented parts included the cerebellum (separate white and grey matter), cerebrum (separate white and grey matter) and brain stem, while image filters were employed to smooth regions within masks, to edit the morphology and to fill cavities. Boolean operations were used to remove any overlapping masks. Tools for 'confidence connected region growing' (CCRG) and 'magnetic lasso' were particularly suitable, in this instance, for capturing regions including the skull, vertebrae and ventricles. The CCRG tool functions by selecting a seed point before building a region of neighbouring voxels based on their similarity to the original seed point. The magnetic lasso tool used for segmentation also has a propagation option that allows the outline of a region to be tracked to the next image slice. A technique that uses existing parts to help build neighbouring parts was also applied to the model, which enabled the generation of the tentorium cerebelli by creating a one voxel thick layer on the superior surface of the cerebellum. The final bitmapped (voxel) images were anti-aliased and smoothed to reproduce the smooth contours of the biological structures. Proprietary multi-part algorithms in ScanIP were used for this purpose to ensure that no changes in connectivity or the volume of the smoothed structures took place. This technique reproduces the accuracy of the scan data.

Table 1. List of anatomical structures in current head model.

Structures differentiated, defined as separate element sets.		
1 Skin 2 Muscles 3 Soft tissues 4 Skull inner and outer table 5 Skull dipole 6 Mandible 7 Cervical vertebrae 8 Intervertebral discs 9 CSF 10 Frontal sinus 11 Maxillary sinus	12 Cerebrum – grey matter 13 Cerebellum – grey matter 14 Cerebrum – white matter 15 Cerebellum – white matter 16 Falx cerebri 17 Tentorium cerebella 18 Eyes 19 Optic nerves 20 Brain stem – medulla 21 Brain stem – midbrain 22 Brain stem - pons	23 Spinal cord 24 Ventricles – lateral (right) 25 Ventricles – lateral (left) 26 Ventricles – third 27 Ventricles – fourth 28 Ventricles – aqueduct of Sylvius 29 Ventricles – foramen of Monro 30 Venous sinuses and bridging veins 31 Venous sinuses and bridging veins walls (shell elements) 32 Dura mater (shell elements) 33 Sclera (eyes) (shell elements)

Step 3: Image enrichment and modification: Following segmentation, the image data was enriched by incorporating CAD models of structures where the original greyscale contrast made it impossible to distinguish between structures. Facial and neck muscles were imported from a Standard Tessellation Language (STL) surface triangulation library. ScanIP module +CAD was used to scale and position parts, and to convert them into image masks using a process called 'voxelisation', whereby a distance function is used to calculate representative greyscale

information. This technique also means that it is straightforward to modify original segmented data to incorporate new structures such as helmets and probes, and to introduce pathologies or combine different structures into one.

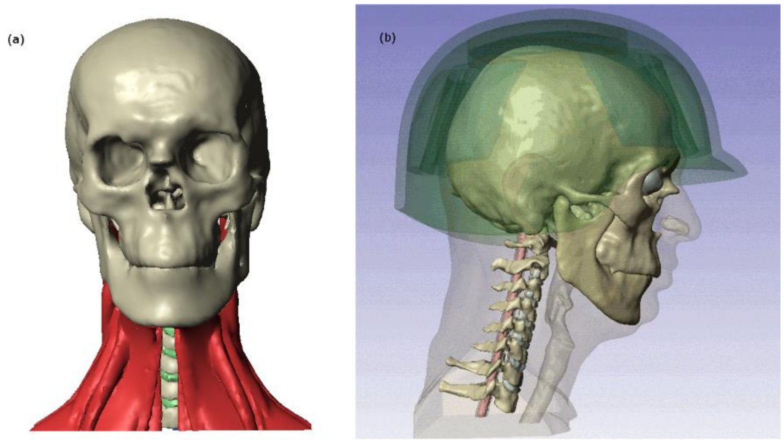

Figure 2. Example of image enrichment: (a) introduction of neck muscles from external CAD source, (b) example of a modification incorporating a helmet design.

Step 4: Image-based mesh generation: After segmentation, the image data can be converted into a mesh using two routes. The first approach involves directly converting ROIs into volumetric FE models by using a multi-part Extended Volumetric Marching Cubes (EVOMAC) approach (Young et al, 2008). Alternatively, the boundaries of the voxelised ROIs can be converted into surface representations (such as triangulated surfaces (STL/NURBS) and used as the basis for mesh generation using a range of automated mesh-generation algorithms. Both mesh generation techniques were explored, incorporating the EVOMAC-based mesher and a multi-part surface decimation algorithm followed by a mixed Delaunay advancing front approach (Young et al, 2008).

The EVOMAC-based approach produces a structured mesh composed of both hexahedral and tetrahedral elements, or purely of tetrahedral elements. The second approach results in unstructured, fully tetrahedral meshes (see Figure 4), that can be modified by controlling element sizes and the final element count. The NRL-Simpleware head model used for simulation of Traumatic Brain Injury was generated as an unstructured, all tetrahedral mesh consisting of 3.72 M volumetric elements, with options remaining for new meshes to be created from the pre-segmented data.

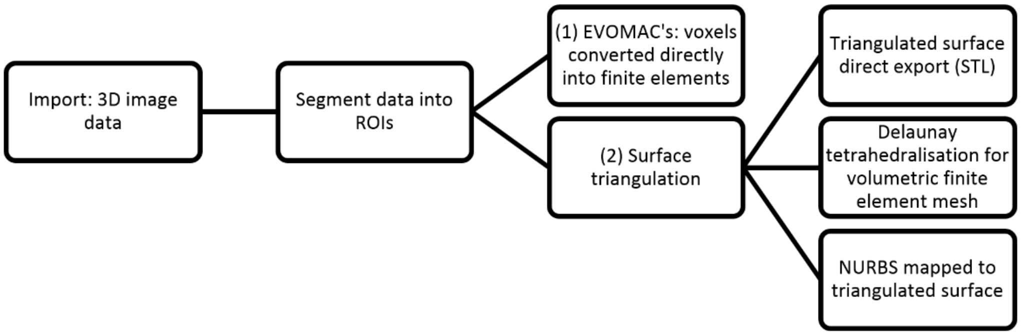

Figure 3. Model generation procedure following image acquisition

Other mesh modification options that can be applied before simulation include: specifying contact pairs to allow for sliding surfaces or separation; adding node and surface sets based on mask geometry or in arbitrary user-defined regions; defining material properties based on the underlying greyscale intensity of the image; and applying Boolean operations directly to structures in image space to merge or remove features or specific regions, reducing the element count if a distinction is not required.

Figure 4. Sagittal section of the unstructured, all tetrahedral mesh with 3.72 M volumetric elements: (left) oblique view (right) normal view.

4. Adaptation of prototype model for Abaqus simulation

The NRL-Simpleware model was developed using meshing techniques suitable for converting pre-segmented data into FE models for different applications. In this context, the main unstructured mesh used for the model was adapted into a mixed-element mesh to simulate head injury under mid-to high-rate impact and blast loading conditions. Four-node linear elements were initially used as a computationally inexpensive option, but required modification as they are stiffer than hexagonal elements, and are liable to experience volumetric locking, making them unsuitable for displacement-based FE formulations and modelling near-incompressible materials such as the brain.

Hybrid elements capable of describing pressure as an independently interpolated solution variable one degree lower than displacement degrees of freedom were considered, but are not available in Abaqus/Explicit. By comparison, 10-node quadratic tetrahedral elements (used in Abaqus/Explicit) avoid locking and allow high-fidelity geometric representations, but are computationally expensive. To ensure high-rate simulations, a compromise was made between computational efficiency and accuracy by building the mesh with regions of near-incompressible materials, such as the cerebrospinal fluid (CSF) and the brain, with quadratic elements. Changes in nodal definitions were performed to describe the interface of the quadratic and linear parts of the FE mesh, including splitting shared nodes between quadratic and linear elements to prevent co-penetration of the additional nodes on the quadratic side into the linear elements, and defining contact interactions at these interfaces.

Linear elements were converted into quadratic elements to build regions of near-incompressible materials such as the brain, spinal cord, CSF, sinuses filled with air, ventricles filled with CSF, veins filled with fluid, and eyes. Contact surfaces were created between quadratic elements of veins and linear elements of skull, veins and soft tissue outside the intracranial region, and at the eyes and soft tissue/skin, by duplicating shared nodes at interfaces. Tied contact conditions were also imposed at these interfaces, and the skull and mandible partitioned into multiple regions with similar outward facing normal vectors, allowing transversely isotropic material properties to be assigned to each region.

In addition, tied contact conditions were imposed between the sub-arachnoid region filled with CSF, and the *dura mater/pia mater*. Conditions were also imposed for the spinal cord, where appropriate, with material models for individual parts based on experimental data whenever available. The functional forms of models included simple linear elastic and equations of state, as well as more advanced hyper-viscoelastic models. A modified Monte Carlo-based optimisation scheme was used for calibration of these complex models. More details on constitutive models, calibration and verification and validation are available (Kota et al, 2014).

5. Applications

The adapted NRL/Simpleware model was used for blunt impact (low-to-mid rate) and blast overpressure (mid-to-high rate) simulations. Abaqus/Explicit was chosen for running simulations using 200 Intel® cores (2GB RAM/core; 2.6 GHz core speed) on an SGI Ice X system. A variable mass-scaling scheme was used, resulting in a reasonable time increment of 50 ns or more during simulation; this allowed the completion of around 20 ms of total simulation time in 24 hours. Change of total model mass during simulations was checked and recorded as being lower than 0.09% throughout, indicating that no significant effect on inertial characteristics took place.

The blunt impact loading application was validated against results from an experiment performed on a post-mortem human subject (Nahum et al, 1977) to reproduce automotive impact. The experiment (#37 in the original study) involved a frontal impact to the head at 45° by a padded impactor of 5.6 kg mass travelling at 9.94 m/s (Figure 5). Simulations were run using the experimental force recorded on the head as the input to the model, with no other boundary conditions applied. The predicted intracranial pressures were compared with experimental data for frontal and parietal regions (Figure 6 (a) and (b)). The simulated pressures in the model reasonably capture the pressure histories recorded within the skull.

Using this computational modelling approach enables a build-up of detailed spatial data that is otherwise typically not practical to collect from experiments. Post-processing of the simulation data can, for example, be performed to quantify the injured brain volume as a function of event time based on injury threshold measures described in the literature for focal and diffuse injuries (Bešenski, 2002). For the current simulation, Python scripting was used to calculate the evolution of these volumes from the large output database. For example, the temporary history for focal injury volume was based on a pressure threshold of 173 kPa (Zhang et al, 2004). Diffuse injury volume was based on a shear strain threshold of 5% (Margulies and Thibault, 1992), as shown in Figure 6 (c), with post-processing capabilities highlighting the utility of the computational models.

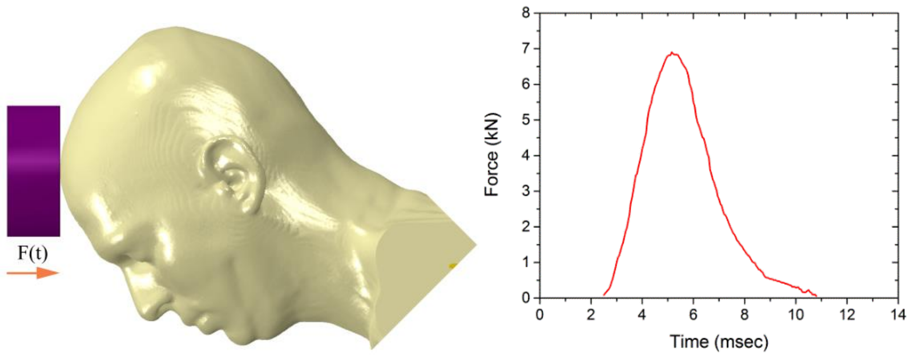

Figure 5. (left) Schematic of a padded impactor hitting the head model at 45° angle; (right) instead of the impactor, the experimental force-time plot was used.

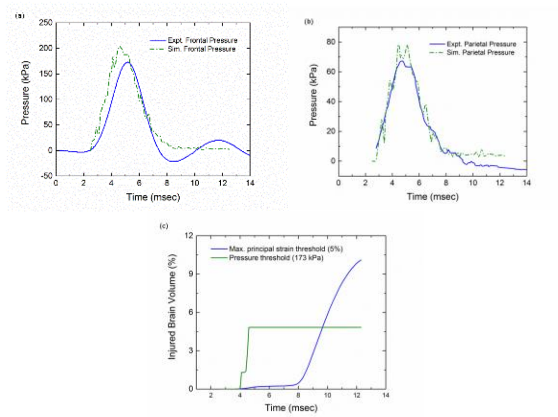

Figure 6. Comparison between experimental and predicted pressures for blunt impact to the head in (a) frontal and (b) parietal regions of the brain, respectively; (c) Temporal history of injured brain volume based on maximum principal strain threshold of 5% and pressure threshold of 173 kPa.

Blast overpressure loading was simulated by choosing the incident wave-loading option in Abaqus/Explicit. The magnitude of the applied pressure pulse is specified on a plane with a specific normal vector; as the wave progresses in the direction of the normal, it encounters the target in a manner similar to a true overpressure impact. However, this does not allow for the wraparound effect. A frontal loading with a Friedlander wave profile (Dewey, 2010) was chosen for this study, with a peak pressure of approximately 430 kPa (Figure 7). The passage of the pressure wave passing across the face and close to the mid-sagittal plane of the head is shown in Figure 8.

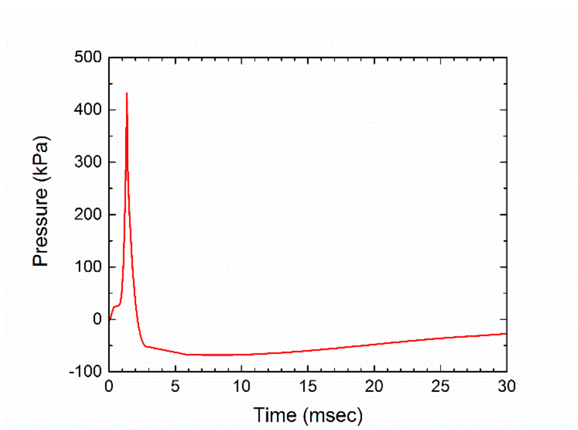

Figure 7. Friedlander wave profile used in frontal blast loading simulation.

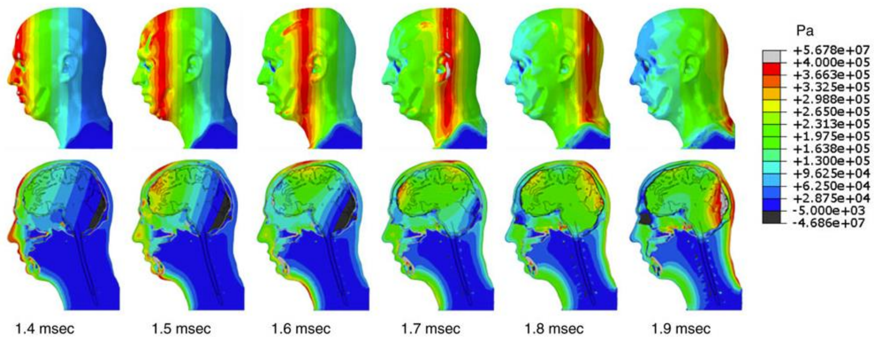

Figure 8. Passage of peak pressure pulse across the face and near mid-sagittal plane of the head during loading.

The injurious effect of this pressure pulse can be displayed in a temporal-spatial form by collecting the temporal injury data for each individual material point and plotting it over the target volume. These graphics can then be used to predict injury patterns or to draw spatial comparisons amongst different metrics of injury to determine their relative effectiveness in predicting actual injury. For example, brain regions based on thresholds of 11 kPa effective stress (Kang et al, 1997) for focal injury, and 5% maximum principal strain (Margulies and Thibault, 1992) for diffuse injury, are highlighted in Figure 9 (a) and (b). The red-coloured regions represent cumulative injury in the first 5 ms based on each threshold.

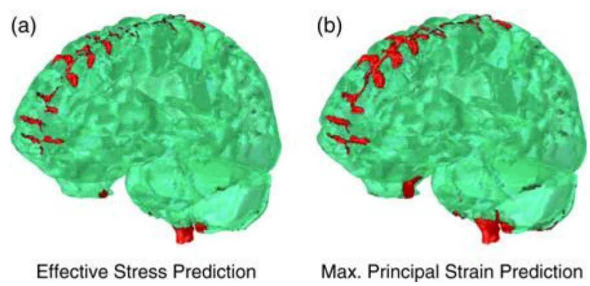

Figure 9. Spatial identification of injured brain regions due to blast overpressure loading based on (a) effective stress threshold of 11 kPa for focal injury and (b) maximum principal strain threshold of 5% for diffuse injury, up to 5 ms. Red-coloured regions have experienced values beyond the respective thresholds.

6. Summary

The NRL-Simpleware head model was developed using novel image-based segmentation and meshing techniques for simulation in Abaqus/Explicit. By generating meshes from pre-segmented data, the approach represents a breakthrough in terms of flexibility compared to previous FE modelling methods. Users are able to adapt models to suit different simulation needs, with options available for incorporating new structures of interest, cropping extents of interest and merging features together. In addition, the ability to introduce robust contact surface definitions at the interface between parts, and to locally refine or decimate meshes, makes it straightforward to customise models for different applications.

Simulations using the NRL-Simpleware head model that recreated experimental data (Nahum et al, 1977) showed excellent agreement with benchmark results for blunt impact. Blast overpressure simulation results that reproduced conditions associated with military and explosive weaponry also demonstrated the head models' capabilities for predicting brain injury as a function of both location and time. This success opens up the use of biofidelic head models for future simulations in Abaqus.

The approach outlined in this paper is capable of generating more detailed structures from the head and brain geometry, but is currently limited by the number of elements that can be reasonably solved by solvers using existing, and cost-effective, computational resources. As imaging and simulation techniques develop, the image-based segmentation and mesh generation techniques this paper proposes will be easily adaptable and scalable to new challenges. Future investigations might include generating a population of head models from image data used to study variations in anatomy according to impact response. Other challenges for future research include more accurately representing the highly complex features of hard and soft tissue structures.

7. References

1. Abaqus Documentation, 2012. Dassault Systémes Simulia Corp., Providence, RI.
2. Bešenski N., "Traumatic injuries: imaging of head injuries," Eur Radiol., 12(6), 1237-1252, 2002.
3. Chen, Y., and M. Ostoja-Starzewski, "MRI-based finite element modeling of head trauma: spherically focusing shear waves,'' Acta Mech., 213, 155-167, 2010.
4. Dewey, J.M, "The shape of the blast wave: studies of the Friedlander equation," 21st international symposium on military aspects of blast and shock, Israel, 2010.
5. Kang, H.S., R. Willinger, B.M. Diaw, and B. Chinn, "Validation of a 3D anatomic human head model and replication of head impact in motorcycle accident by finite element modeling," SAE Trans., 106(6), 3849-3858, 1997.
6. Kota, N., A. Bagchi, and S.M. Qidwai, "On the challenges in verification and validation of biomechanical models of humans: a case study on head model development for impact loading," J Biomech, 2014.
7. Kraft, R., P. Mckee, A. Dagro, and S. Grafton, "Combining the finite element method with structural connectome-based analysis for modeling neurotrauma: connectome neurotrauma mechanics," PLoS Comput Biol. (Internet), Available from: http://dx.plos.org/1-.1371/journal.pcbi.1002619, 2012.

8. Margulies, S.S., and L.E. Thibault, “A proposed tolerance criterion for diffuse axonal injury in man,” J Biomech, 25(8), 917-923, 1992.
9. Mehta, B.V., S. Rajani, and G. Sinha, “Comparison of image processing techniques (magnetic resonance imaging, computed tomography scan and ultrasound) for 3D modeling and analysis of the human bones,” J Digit. Imaging, 10, 203-206, 1997.
10. Nahum, A.M., R. Smith, and C.C. Ward, “Intracranial pressure dynamics during head impact,” Proceedings of the 21st Stapp Car Crash Conference, 339-366, 1977.
11. Takhounts, E.G. S. Ridella, V. Hasija, R.E. Tannous, J.Q. Campbell, D. Malone, et al., “Investigation of traumatic brain injuries using the next generation of simulated injury monitor (SIMon) finite element head model,” Stapp Car Crash J., 52, 1-31, 2008.
12. U.S. Department of Veterans Affairs, Traumatic brain injury: a guide for patients (Internet), Available from: http://www.mentalhealth.va.gov/docs.tbi.pdf
13. Young, P.G., T.B.H. Beresford-West, S.R.L. Coward, B. Notarberadino, B., and A. Abdul-Aziz, “An efficient approach to converting three-dimensional image data into highly accurate computational models,” Philos Teans R Soc A Math Phys Eng Sci, 366, 3155-3173, 2008.
14. Zhang, L., K.H. Yang, A.I. King, “A proposed injury threshold for mild traumatic brain injury,” J Biomech Eng, 126(2), 226-236, 2004.

8. Acknowledgement

Research was carried out at Simpleware Ltd. and the US Naval Research Location. Funding was supported by the Office of Naval Research (ONR) through the US Naval Research Laboratory’s Basic Research Program, and the Department of Defense (DoD) High Performance Computing Modernization Program (HPCMP) using the Air Force Research Laboratory (AFRL) Major Shared Resource Center (MSRC) under project 416, subproject 231.